

## Analysis of neutron + nucleus scattering data with nonlocal optical potentials based on the resonating-group formulation

T. Kaneko\*

*Theoretical Physics Institute, School of Physics, University of Minnesota, Minneapolis, Minnesota 55455  
and Department of Physics, Niigata University, Niigata 950-21, Japan*

M. LeMere

*566 Lincoln Avenue, Los Altos, California 94022*

Y. C. Tang

*School of Physics, University of Minnesota, Minneapolis, Minnesota 55455*

(Received 10 February 1992)

A nonlocal optical model is used to analyze the scattering of neutrons by  $^{12}\text{C}$ ,  $^{16}\text{O}$ ,  $^{28}\text{Si}$ ,  $^{32}\text{S}$ , and  $^{40}\text{Ca}$  in the energy region from about 13 to 40 MeV. The real part of the internuclear interaction is obtained by using the prescription of a recently proposed nucleon + nucleus model  $K$ , which is a microscopic model based on the resonating-group formulation. A simple approximation, called the spherical approximation, is introduced to treat the cases involving non-closed-subshell target nuclei. The imaginary part used is purely phenomenological, and is obtained by simply adopting the imaginary potentials which have been found previously by other authors in their analyses with the usual local optical model. The influence of the Perey effect is taken into account by the introduction of an additional multiplicative factor. The results obtained for the differential scattering cross sections and the analyzing powers are quite satisfactory. The essential characteristics of the measured angular distributions are well reproduced. This suggests that model  $K$  is a viable model of great simplicity and can be employed to make systematic and large-scale analyses of all existing nucleon + nucleus scattering data.

PACS number(s): 24.10.-i, 25.40.Dn, 24.10.Ht

### I. INTRODUCTION

The resonating-group method (RGM) has been employed over the last fifty years to study nuclear-structure and nuclear-reaction problems from a microscopic and unified viewpoint (see, e.g., Refs. [1,2]). By utilizing multiple cluster configurations in the formulation [3,4] or by simply introducing phenomenological imaginary potentials to account for effects of open reaction channels [5,6], good agreements between calculations and experiments have generally been obtained. On the other hand, because of analytical complexities in deriving the kernel functions representing the nonlocal internuclear interactions, resonating-group calculations have been limited to light nuclear systems with  $A \lesssim 12$  and a rather small number of selected systems involving heavier nuclei [7]. It is clear that, to extend the domain of practical applicability of the RGM, some simplifying assumptions have to be made. Recently, we have taken an initial step in this direction by considering the nucleon + nucleus case within the RGM framework, but adopting the simplifications of approximating target-recoil effects and taking into account only the direct and the knockon-exchange contributions. The resultant model [8], called model  $K$ , is

then still a microscopic nonlocal model, but possesses the important advantage that the kernel functions for closed-subshell target nuclei can be analytically derived with little difficulty.

The domain of validity for model  $K$  has been carefully examined. By comparing model- $K$  and exact RGM results in the  $n + \alpha$ ,  $n + ^{16}\text{O}$ , and  $n + ^{40}\text{Ca}$  systems for bound-state energies, phase shifts, differential scattering cross sections, and polarizations, it was found [8] that model  $K$  works very well when the nucleon number of the target nucleus is larger than about 10 (see also Ref. [9]) and when the scattering energy is higher than about 10 MeV/nucleon. Thus, model  $K$  covers all the nucleon + nucleus scattering cases that have customarily been analyzed with the usual local optical model [10–12], and, therefore, can be adopted to provide a microscopic understanding of the parameter values which have been phenomenologically determined by this latter model.

There is one important advantage associated with model  $K$  which is especially worth mentioning. This advantage is that the equivalent local potential corresponding to the nonlocal interaction of model  $K$  [13], obtained by using a WKB procedure [14], exhibits already the major part of the energy dependence which was found to be necessary in phenomenological optical-model analyses employing local potentials [10–12]. For example, in the  $n + ^{40}\text{Ca}$  case at 20 and 40 MeV, the volume integrals per nucleon pair of the WKB-equivalent local potentials are equal to 412.5 and 366.8 MeV fm<sup>3</sup>, respectively [13],

---

\*Present and permanent address: Department of Physics, Niigata University, Niigata 950-21, Japan.

which should be compared with the corresponding values of 418.5 and 363.7 MeV fm<sup>3</sup> obtained from a global nucleon + nucleus optical-model potential called the CH-89 potential [10]. Thus, for this energy range, model *K* yields a respectable 83% of the empirically determined energy dependence. This suggests, therefore, that when model *K* is used to analyze the experimental data, the real part of the internuclear interaction can be chosen to be explicitly energy independent, thereby reducing the number of adjustable parameters which are required in the analysis.

In this investigation, we use model *K* to analyze the scattering data of neutrons by the target nuclei <sup>12</sup>C, <sup>16</sup>O, <sup>28</sup>Si, <sup>32</sup>S, and <sup>40</sup>Ca in the c.m. energy region between about 13 and 40 MeV. The main purpose is, of course, to examine the general utility of this model in studying experimental results. For the cases with <sup>16</sup>O and <sup>40</sup>Ca, the expressions for the direct potentials and knockon-exchange kernel functions given in Ref. [8] can be immediately adopted, because these particular nuclei can be considered to be well described by closed proton and neutron subshell configurations. The situation is somewhat different when the target nucleus is <sup>12</sup>C, <sup>28</sup>Si, or <sup>32</sup>S. For these nuclei, the higher (*nl*) subshells are not completely filled; hence, further considerations must be made in order to render model *K* applicable. Prompted by our desire to keep model *K* as simple as possible, we shall introduce into the calculation an additional approximation, to be called the spherical approximation, which has the

$$\left[ -\frac{\hbar^2}{2\mu} \left( \frac{d^2}{dR^2} - \frac{L(L+1)}{R^2} \right) - E + V^N(R) + \eta_{JL} V^{s.o.}(R) + iW(R) \right] f_{JL}(R) + \int_0^\infty [k_L^N(R, R') + \eta_{JL} k_L^{s.o.}(R, R')] f_{JL}(R') dR' = 0, \quad (1)$$

where  $\mu$  is the reduced mass of the neutron + nucleus system,  $\eta_{JL}$  is given by

$$\eta_{L+1/2, L} = L, \quad \eta_{L-1/2, L} = -(L+1), \quad (2)$$

and  $E$  is the relative energy in the c.m. system. The quantities  $V^N$  and  $V^{s.o.}$  denote the direct nuclear-central and the direct spin-orbit potentials, respectively, while  $k_L^N$  and  $k_L^{s.o.}$  denote the partial-wave nuclear-central and spin-orbit kernel functions representing the knockon-exchange contributions. The expressions for these quantities in the case of closed-subshell target nuclei, such as <sup>16</sup>O and <sup>40</sup>Ca, are given in Ref. [8]. Also, in Eq. (1),  $W(R)$  is a phenomenological imaginary potential which is introduced into the formulation to take into account the effects of reactions on the incident channel.

For the target nuclei <sup>12</sup>C, <sup>28</sup>Si, and <sup>32</sup>S, the expressions for  $V^N$ ,  $V^{s.o.}$ ,  $k_L^N$ , and  $k_L^{s.o.}$  given in Ref. [8] cannot be immediately used, because some of the (*nl*) subshells in these nuclei are not completely filled. In these cases, the straightforward procedure is to derive these expressions, within the framework of model *K*, by using target-nucleus wave functions which have the proper proton and neutron configurations to yield the observed proper-

desirable consequence that the expressions given in Ref. [8] can be readily adapted to the case involving a non-closed-subshell target nucleus. In the next section, this approximation will be presented, together with an explanation of the plausibility for its adoption.

The nonlocal optical model to be used in this analysis is described in Sec. II. In this model, the real part of the internuclear interaction is based on model *K*, together with the spherical approximation mentioned above. Reaction effects are taken into account by the introduction of a phenomenological imaginary part. In Sec. III, we compare the calculated and experimental results for differential scattering cross sections and analyzing powers. As will be seen there, the agreement is quite satisfactory, thus suggesting that the use of the microscopic model *K* in analyzing experimental data is a good procedure. Finally, in Sec. IV, we discuss the essential findings of this investigation and make some concluding remarks.

## II. THE NONLOCAL OPTICAL MODEL

### A. Brief description of the model

With a nonlocal optical model for neutron + nucleus scattering, one solves the following integro-differential equation for the internuclear radial wave function  $f_{JL}(R)$ :

ties for the ground states of these nuclei. However, this will result in a rather lengthy analytical derivation; hence, for the purpose of preserving the important features of simplicity and generality for model *K*, we shall instead adopt a simple approximation, to be called the spherical approximation, to treat the cases involving non-closed-subshell target nuclei. In this approximation, what we do is to simply multiply the closed-subshell expressions for  $V^N$ ,  $V^{s.o.}$ ,  $k_L^N$ , and  $k_L^{s.o.}$  by a factor equal to  $c_{nl}/N_{nl}$ , where  $c_{nl}$  and  $N_{nl}$  denote the occupation number of nucleons in the (*nl*) subshell and the nucleon capacity of an (*nl*) subshell, respectively. For example, if one chooses the proton configuration in <sup>28</sup>Si to be  $c_{nl} = 2, 6,$  and  $6$  for (*nl*) = (00), (11), and (22), then the (*nl*) = (22) subshell is unfilled, because the capacity  $N_{nl}$  of this subshell is equal to 10, and the contribution to the  $n + ^{28}\text{Si}$  direct spin-orbit potential from the target protons in the (*nl*) = (22) subshell will then be taken to be  $\frac{6}{10} V_{22}^{s.o.}$ , with  $V_{22}^{s.o.}$  given by Eq. (36) of Ref. [8]. In a crude way, one can say that the spherical approximation amounts to omitting the intrinsic deformation of the target nucleus, but treating it as a spherically symmetric system. Macroscopically, the use of the spherical optical model (SOM;

see, e.g., Ref. [15]) to perform systematic analyses of a large body of nucleon + nucleus scattering data can be considered to be acting in the same general spirit.

To discuss the plausibility of the spherical approximation, we first make the following observation. From extensive analysis of nucleon + nucleus scattering data with the phenomenological optical model, it was learned [16] that, in the real nuclear-central potential, the important quantities which dominate the scattering characteristics are the volume integral per nucleon pair  $J_N$  and the rms radius  $R_N$ . With the target-nucleus wave functions constructed in terms of single-nucleon spatial wave functions in a harmonic-oscillator well of width parameter  $\alpha$ , we have found by constructing equivalent local potentials [13] that the contribution to  $J_N$  from the nucleons in an  $(nl)$  subshell depends weakly on the quantum number  $n$  and, for the same value of  $n$ , has almost no  $l$  dependence. In addition to this, the contribution to the mean-square radius of the dominant direct nuclear-central potential also turns out to be  $l$  independent for a given  $n$  value (see Eq. (64) of Ref. [8] and Eq. (18) of Ref. [16]). Based on these considerations, we can state that, from the viewpoint of the elastic-scattering process, the precise way in which nucleons distribute themselves among the various  $l$  states within a major  $n$  shell should

not be of primary importance. To show the validity of this assertion, we shall perform calculations in the  $n + {}^{28}\text{Si}$  and  $n + {}^{32}\text{S}$  cases by adopting target-nucleus configurations which are different in their distributions of nucleons in a particular major shell.

Because of our anticipation that the scattering results will not be greatly sensitive even with respect to the distribution of target nucleons in different  $l$  states within a major  $n$  shell, we are of the opinion that the adoption of the spherical approximation, which is based on the milder assumption of the relative insensitivity of the scattering results with respect to the distribution of nucleons in different magnetic substates within an  $l$  state, should be a reasonable procedure. This is especially so, if we further take into account the important advantage that the resultant model will be so simple as to be suitable for a systematic and large-scale analysis of all existing nucleon + nucleus scattering data in the future.

Using the spherical approximation, one can now easily obtain the expressions for the direct potential and the knockon-exchange kernel functions. As an example, let us consider the case of  $n + {}^{28}\text{Si}$ , with  ${}^{28}\text{Si}$  having proton and neutron configurations specified by  $c_{nl} = 2, 6, \text{ and } 6$  for  $(nl) = (00), (11), \text{ and } (22)$ . With a nucleon-nucleon potential having the basic form

$$V_{ij} = -V_0 \exp(-\kappa r_{ij}^2) (w - mP_{ij}^\sigma P_{ij}^\tau + bP_{ij}^\sigma - hP_{ij}^\tau) - \frac{1}{2\hbar} V_\lambda \exp(-\lambda r_{ij}^2) (\sigma_i + \sigma_j) \cdot (\mathbf{r}_i - \mathbf{r}_j) \times (\mathbf{p}_i - \mathbf{p}_j), \quad (3)$$

the results are as follows:

$$V^N(R) = -V_0(4w - m + 2b - 2h) \left( \frac{\alpha}{\alpha + \kappa} \right)^{3/2} \times \left[ \frac{7\alpha^2 + 5\alpha\kappa + \kappa^2}{(\alpha + \kappa)^2} + \frac{2\alpha\kappa^2(3\alpha + \kappa)}{(\alpha + \kappa)^3} R^2 + \frac{4\alpha^2\kappa^4}{5(\alpha + \kappa)^4} R^4 \right] \exp \left[ -\frac{\alpha\kappa}{\alpha + \kappa} R^2 \right], \quad (4)$$

$$K^N(\mathbf{R}, \mathbf{R}') = -V_0(-w + 4m - 2b + 2h) \left( \frac{\alpha}{\pi} \right)^{3/2} \{ 1 + 2\alpha \mathbf{R} \cdot \mathbf{R}' + \frac{2}{5}\alpha^2 [3(\mathbf{R} \cdot \mathbf{R}')^2 - R^2 R'^2] \} \times \exp \left[ -\left( \frac{\alpha}{2} + \kappa \right) (R^2 + R'^2) + 2\kappa \mathbf{R} \cdot \mathbf{R}' \right], \quad (5)$$

$$V^{s.o.}(R) = -2J_\lambda \alpha^{5/2} (-1 + \frac{2}{5}\alpha R^2 + \frac{4}{5}\alpha^2 R^4) \exp(-\alpha R^2), \quad (6)$$

and  $K^{s.o.}(\mathbf{R}, \mathbf{R}')$  obtained by using Eq. (54) of Ref. [8]. In deriving Eq. (6), we have adopted a zero-range approximation by letting the spin-orbit range parameter  $\lambda$  approaching infinity. As a consequence of this approximation, the nucleon-nucleon spin-orbit potential is then characterized by a single parameter  $J_\lambda$  given by

$$J_\lambda = V_\lambda \lambda^{-5/2}. \quad (7)$$

In the actual analysis, we have used the Minnesota (MN) potential given by Eqs. (65)–(67) of Ref. [8]. This potential has a somewhat more complicated central part than the nucleon-nucleon potential of Eq. (3). We should emphasize, however, that this does not cause any problem. The calculation can still be readily carried out by

making only trivial modifications of the expressions given in Ref. [8] for the direct potentials and the knockon-exchange kernel functions.

#### B. Choice of parameters in the real part of the internuclear interaction

The real part of the internuclear interaction is represented by the direct potentials and the knockon-exchange kernel functions that involve three parameters. These parameters are (i) the width parameter  $\alpha$  of the harmonic-oscillator well which provides the single-nucleon wave functions for the target nucleus, (ii) the exchange-mixture parameter  $u$  in the nuclear-central part of the MN nucleon-nucleon potential, and (iii) the spin-

orbit strength parameter  $J_\lambda$  defined by Eq. (7) in the preceding subsection. In the following, we shall discuss the ways in which we assign values to these three parameters in the cases of neutron scatterings by the target nuclei  $^{12}\text{C}$ ,  $^{16}\text{O}$ ,  $^{28}\text{Si}$ ,  $^{32}\text{S}$ , and  $^{40}\text{Ca}$ .

The width parameter  $\alpha$  is determined by using empirical information on the rms charge radius of the target nucleus [17]. By choosing the lowest configurations for the various target nuclei, the resultant values for  $\alpha$  turn out to be equal to 0.389, 0.334, 0.306, 0.290, and 0.253  $\text{fm}^{-2}$  for  $^{12}\text{C}$ ,  $^{16}\text{O}$ ,  $^{28}\text{Si}$ ,  $^{32}\text{S}$ , and  $^{40}\text{Ca}$ , respectively.

The parameters  $u$  and  $J_\lambda$  in the nucleon-nucleon potential are chosen by using information which is available from exact single-configuration RGM calculations in the  $n + \alpha$ ,  $n + ^{16}\text{O}$ , and  $n + ^{40}\text{Ca}$  cases. By best fitting the bound-state or resonance energies, it was found [18] that the  $u$  values should be taken to be 0.970, 0.924, and 0.856 in these three systems, respectively, and  $J_\lambda$  can assume a constant value of 50  $\text{MeV fm}^5$ . Then, by adopting a simple interpolation procedure, we decide to use  $u = 0.938$ , 0.924, 0.887, 0.876, and 0.856 in the  $n + ^{12}\text{C}$ ,  $n + ^{16}\text{O}$ ,  $n + ^{28}\text{Si}$ ,  $n + ^{32}\text{S}$ , and  $n + ^{40}\text{Ca}$  systems, respectively, and a common value of  $J_\lambda = 50 \text{ MeV fm}^5$  in all these systems. The finding that  $u$  needs to be system dependent and slowly decreasing with the nucleon number of the compound nucleus is likely a consequence of the fact that our chosen nucleon-nucleon potential has only a weak repulsive core and does not quite satisfy the requirement of saturation.

### C. Choice of parameters in the imaginary part of the internuclear interaction

Since the main purpose of this investigation is not to obtain detailed fittings of the neutron + nucleus scattering data, but to study the general utility of model  $K$  in providing the real part of the internuclear interaction, we shall adopt a very simple recipe for the imaginary part  $W(R)$ . What we do for a particular scattering system at a given energy is to write

$$W(R) = \tilde{C}_p W_{\text{opt}}(R), \quad (8)$$

where  $W_{\text{opt}}(R)$  represents the phenomenological imaginary potential already obtained by other authors in their analysis of the experimental data with the usual local optical model, and  $\tilde{C}_p$  is a multiplicative factor to be called the Perey factor. It is necessary to introduce this multiplicative factor, because it has been found that, in the region of strong interaction, the magnitude of the relative-motion wave function in a nonlocal potential is consistently smaller than that determined from a phase-equivalent local potential (i.e., the so-called Perey effect) [6,19,20].

The Perey factor  $\tilde{C}_p$  will be chosen in the following manner. We consider the  $n + ^{40}\text{Ca}$  system as a typical case, and calculate the total reaction cross section  $\sigma_R$  when the real part of the internuclear interaction is given by either the nonlocal potential of model  $K$  or its equivalent local potential through a WKB procedure. With imaginary potentials of pure surface geometry, we find that, to reproduce the  $\sigma_R$  values in the local case,

TABLE I. Perey factor and references for  $W_{\text{opt}}$  used in the analysis of neutron + nucleus scattering data.

Target nucleus	$E$ (MeV)	$\tilde{C}_p$	Refs. for $W_{\text{opt}}$
$^{12}\text{C}$	16.8	1.20	[21]
	24.0	1.15	[22]
$^{16}\text{O}$	16.94	1.20	[23]
	21.65	1.15	[24]
$^{28}\text{Si}$	13.5	1.20	[25]
	29.26	1.10	[15]
$^{32}\text{S}$	13.58	1.20	[25]
	39.08	1.10	[22]
$^{40}\text{Ca}$	13.56	1.20	[26]
	29.3	1.10	[27]

one must introduce in the nonlocal case multiplicative factors  $\tilde{C}_p$  equal to 1.15, 1.09, and 1.05 at  $E = 20, 40,$  and  $60 \text{ MeV}$ , respectively. When volume absorptions are used, similar features are found although  $\tilde{C}_p$  turns out to be slightly larger. The finding that  $\tilde{C}_p$  decreases with energy and converges toward unity simply reflects the fact that, as the energy increases from 20 to 60 MeV, the knockon contribution, which gives rise to the nonlocal part of the interaction, becomes effectively weaker in relation to the direct contribution which is represented by a totally local potential.

In Table I, we list the Perey factors  $\tilde{C}_p$  used in the analysis and the references in which the absorptive potentials  $W_{\text{opt}}$  appear. The values of  $\tilde{C}_p$  are chosen according to the information learned in the  $n + ^{40}\text{Ca}$  case discussed above, and have not been fine tuned to obtain best fits with measured results.

## III. ANALYSIS OF NEUTRON + NUCLEUS SCATTERING DATA

With the parameters chosen according to the discussion given in the preceding section, we calculate the differential scattering cross sections  $\sigma(\theta)$  and the analyzing powers  $A_y(\theta)$  in the  $n + ^{12}\text{C}$ ,  $n + ^{16}\text{O}$ ,  $n + ^{28}\text{Si}$ ,  $n + ^{32}\text{S}$ , and  $n + ^{40}\text{Ca}$  cases. The results in the energy region from about 13 to 40 MeV are shown by the solid curves in Figs. 1–5 for  $\sigma(\theta)$  and in Figs. 6–8 for  $A_y(\theta)$ . To obtain these results, we have adopted the same configurations for the protons and the neutrons in the target nuclei. These configurations are  $(1s)^2(1p)^4$  for  $^{12}\text{C}$ ,  $(1s)^2(1p)^6$  for  $^{16}\text{O}$ ,  $(1s)^2(1p)^6(1d)^6$  for  $^{28}\text{Si}$ ,  $(1s)^2(1p)^6(1d)^6(2s)^2$  for  $^{32}\text{S}$ , and  $(1s)^2(1p)^6(1d)^{10}(2s)^2$  for  $^{40}\text{Ca}$ , where the spectroscopic notations  $1s$ ,  $1p$ ,  $1d$ , and  $2s$  denote the single-nucleon configurations in a harmonic-oscillator well with  $(nl) = (00)$ ,  $(11)$ ,  $(22)$ , and  $(20)$ , respectively. In the  $n + ^{28}\text{Si}$  and  $n + ^{32}\text{S}$  cases, we have additionally performed calculations with  $^{28}\text{Si}$  assumed to have the configuration  $(1s)^2(1p)^6(1d)^4(2s)^2$  and with  $^{32}\text{S}$  assumed to have the configuration  $(1s)^2(1p)^6(1d)^8$ . The results obtained with these configurations are shown by the dashed curves in Figs. 3, 4, and 7.

First, we discuss the comparisons of the calculated  $\sigma(\theta)$  results with experimental data (solid circles, Refs.

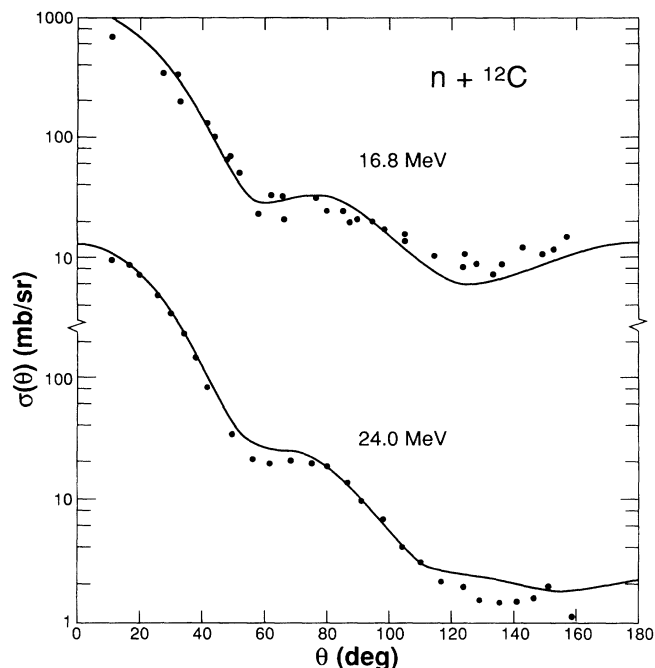


FIG. 1. Comparison of calculated and experimental differential cross sections for  $n + {}^{12}\text{C}$  scattering at 16.8 and 24.0 MeV. Experimental data shown are those of Refs. [23,28].

[15, 22–28]). By examining Figs. 1–5, we can make the following statements.

(i) The agreement between calculation and experiment is quite satisfactory. From these figures, one can see that

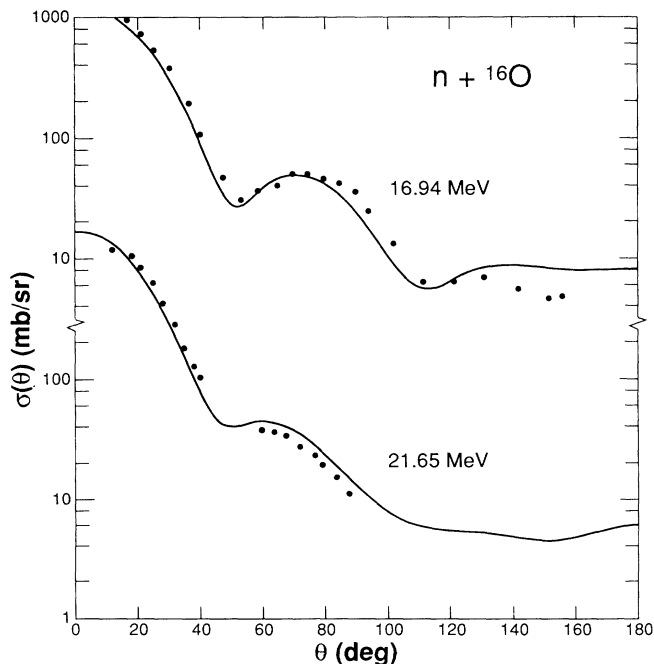


FIG. 2. Comparison of calculated and experimental differential cross sections for  $n + {}^{16}\text{O}$  scattering at 16.94 and 21.65 MeV. Experimental data shown are those of Refs. [23,24].

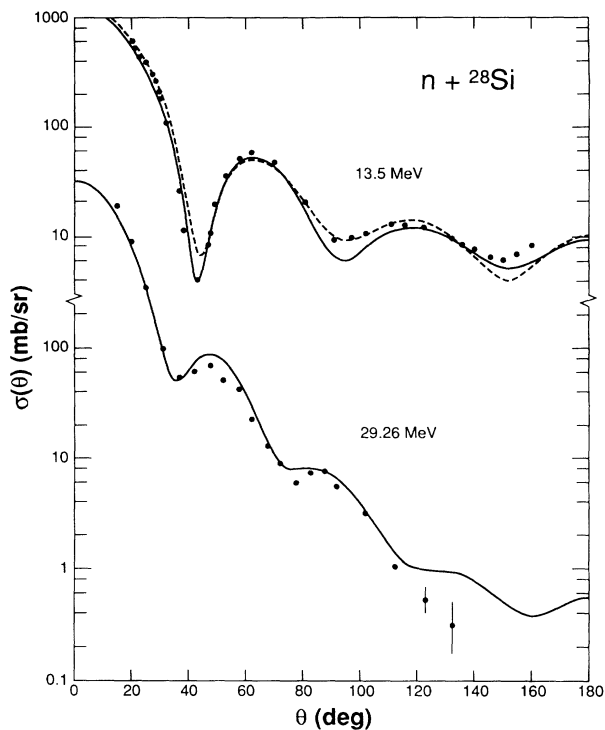


FIG. 3. Comparison of calculated and experimental differential cross sections for  $n + {}^{28}\text{Si}$  scattering at 13.5 and 29.26 MeV. The solid and dashed curves represent results obtained when  ${}^{28}\text{Si}$  is described by the configurations  $(1s)^2(1p)^6(1d)^6$  and  $(1s)^2(1p)^6(1d)^4(2s)^2$ , respectively. Experimental data shown are those of Ref. [15].

the calculation correctly yields the oscillatory features of the experimental angular distributions and the general magnitudes of the measured cross sections.

(ii) The quality of fit obtained with the present nonlocal model is rather similar to that obtained with the phenomenological spherical optical model (SOM) which contains an energy-dependent real-central local potential.

(iii) The quality of the calculated cross-section results in the  $n + {}^{12}\text{C}$ ,  $n + {}^{28}\text{Si}$ , and  $n + {}^{32}\text{S}$  cases which involve nonclosed-subshell target nuclei is comparable to that in the  $n + {}^{16}\text{O}$  and  $n + {}^{40}\text{Ca}$  cases which involve closed-subshell target nuclei. This is an indication that the adoption of the spherical approximation is a reasonable simplifying procedure.

(iv) Cross-section results obtained with different target configurations in the  $n + {}^{28}\text{Si}$  and  $n + {}^{32}\text{S}$  cases, represented by solid and dashed curves in Figs. 3 and 4, are seen to be different in relatively minor ways. This shows that, at least for the differential scattering cross sections, the result is mainly sensitive to gross properties of the internuclear interaction, such as the volume integral per nucleon pair and the rms radius [16], but much less so to the detailed structure of the target nucleus, such as the distribution of nucleons among various  $l$  states in a major shell.

At 13.5 MeV, the calculated total cross sections  $\sigma_T$  in the  $n + {}^{28}\text{Si}$ ,  $n + {}^{32}\text{S}$ , and  $n + {}^{40}\text{Ca}$  cases, with  ${}^{28}\text{Si}$  and  ${}^{32}\text{S}$  assumed to have the configurations  $(1s)^2(1p)^6(1d)^6$  and  $(1s)^2(1p)^6(1d)^6(2s)^2$ , are equal to 1766, 1972, and 2136

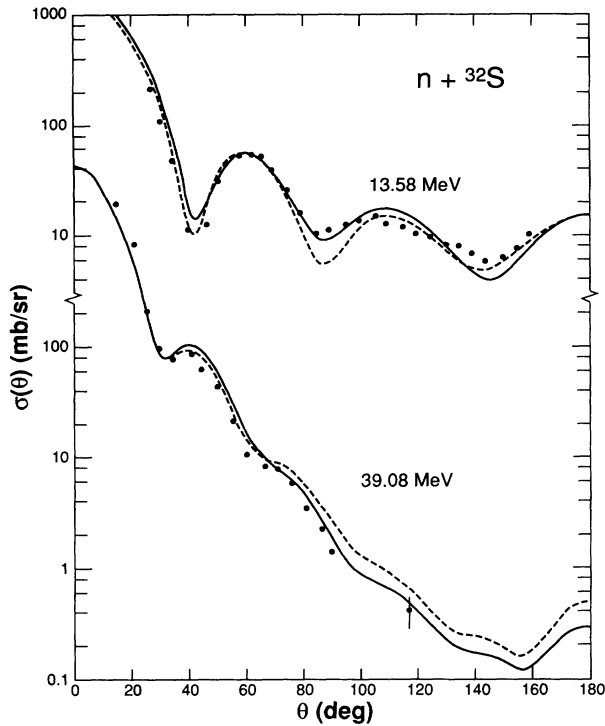


FIG. 4. Comparison of calculated and experimental differential cross sections for  $n + {}^{32}\text{S}$  scattering at 13.58 and 39.08 MeV. The solid and dashed curves represent results obtained when  ${}^{32}\text{S}$  is described by the configurations  $(1s)^2(1p)^6(1d)^6(2s)^2$  and  $(1s)^2(1p)^6(1d)^8$ , respectively. Experimental data shown are those of Refs. [22,25].

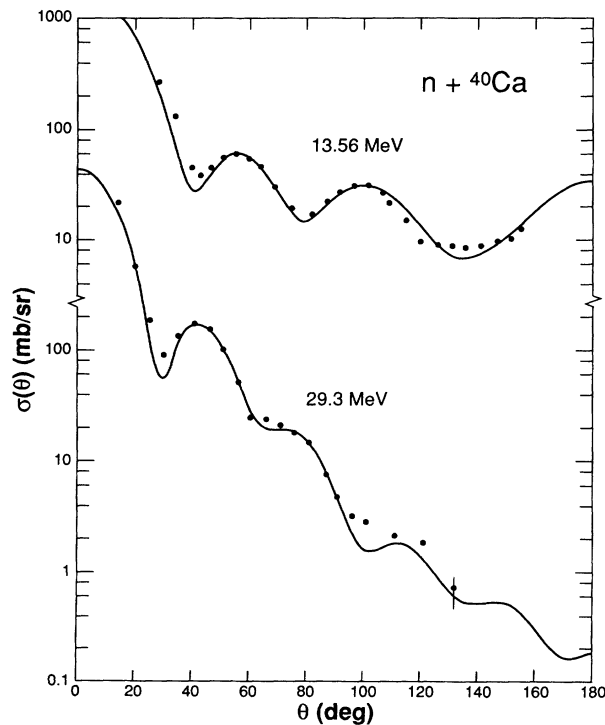


FIG. 5. Comparison of calculated and experimental differential cross sections for  $n + {}^{40}\text{Ca}$  scattering at 13.56 and 29.3 MeV. Experimental data shown are those of Refs. [26,27].

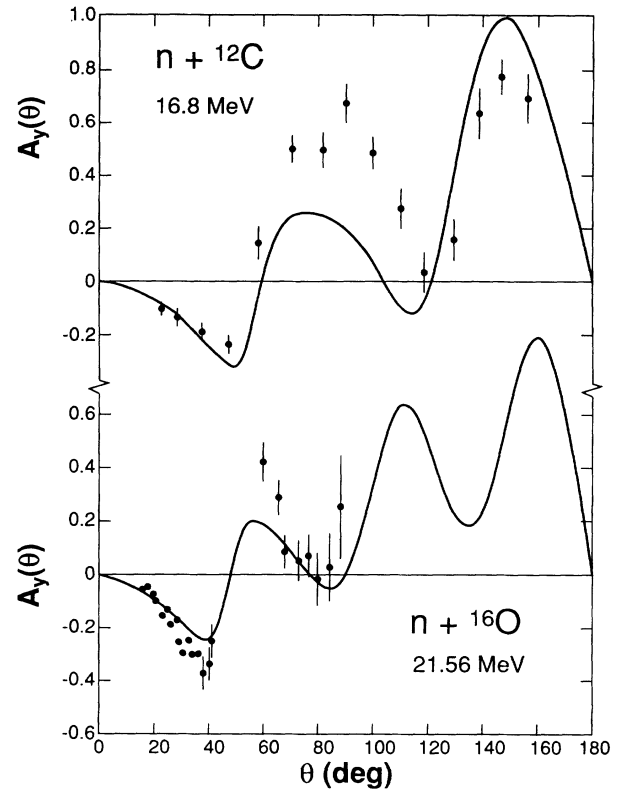


FIG. 6. Comparison of calculated and experimental analyzing powers for  $n + {}^{12}\text{C}$  scattering at 16.8 MeV and for  $n + {}^{16}\text{O}$  scattering at 21.56 MeV. Experimental data shown are those of Refs. [21,24].

mb, respectively. These  $\sigma_T$  results agree well with the measured values obtained by Foster and Glasgow [29]. When one chooses instead the configurations of  ${}^{28}\text{Si}$  and  ${}^{32}\text{S}$  to be  $(1s)^2(1p)^6(1d)^4(2s)^2$  and  $(1s)^2(1p)^6(1d)^8$ , the corresponding  $\sigma_T$  values are found to change to 1854 and 1872 mb. These changes, being only around 5%, are however rather small, thus leading us to believe that the use of  $\sigma_T$  data as a way to gain information on the structure of the target nucleus is not likely to be a fruitful task.

Calculated analyzing powers are compared with experimental data (solid circles, Refs. [15,21,24–26]) in Figs. 6–8. Here one notes again that the quality of fit is similar to that obtained with the spherical optical model [25]. The calculation correctly yields the essential characteristics of the measured angular distributions, but there is no detailed agreement. In fact, this is not too surprising, because it is known that the analyzing power is more sensitive to the details of the model than the differential scattering cross section. For example, our adoption of a zero-range nucleon-nucleon spin-orbit potential to represent the effects of noncentral forces may be somewhat problematic, and this particular simplification may need to be carefully examined in future investigations.

From Fig. 7, one finds that the analyzing power  $A_y(\theta)$  has a more noticeable dependence on the target-nucleus configuration than the differential scattering cross section  $\sigma(\theta)$ . Again, because of the relatively larger degree of sensitivity of  $A_y(\theta)$  to the details of the model, this is not

entirely unexpected. As one can see from this figure, the general shapes of the analyzing-power curves obtained with the two chosen configurations of the target nucleus are quite similar, but the calculated magnitudes are somewhat different. This indicates that, although the distribution of nucleons among the different  $l$  states in an  $n$  shell does not have a major influence on  $A_y(\theta)$ , one must still pay proper attention to this distribution if a detailed fit to experimental data is desired. In fact, the present finding seems to suggest that one might even use the analyzing-power measurement in an elastic-scattering process as a way to study the structure of the target nucleus. However, we should mention that this may not be a practical suggestion at this moment. It is clear from our discussion above that, for this specific purpose, one must first

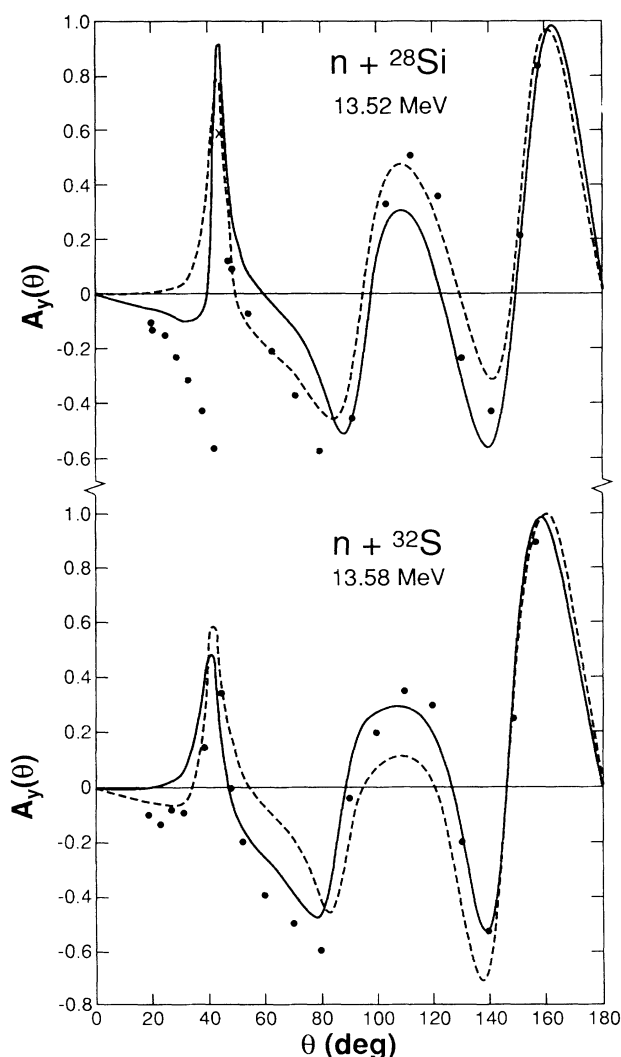


FIG. 7. Comparison of calculated and experimental analyzing powers for  $n + {}^{28}\text{Si}$  scattering at 13.52 MeV and for  $n + {}^{32}\text{S}$  scattering at 13.58 MeV. The solid and dashed curves represent results obtained when  ${}^{28}\text{Si}$  is described by the configurations  $(1s)^2(1p)^6(1d)^6$  and  $(1s)^2(1p)^6(1d)^4(2s)^2$ , respectively, and when  ${}^{32}\text{S}$  is described by the configurations  $(1s)^2(1p)^6(1d)^6(2s)^2$  and  $(1s)^2(1p)^6(1d)^8$ , respectively. Experimental data shown are those of Refs. [15,25].

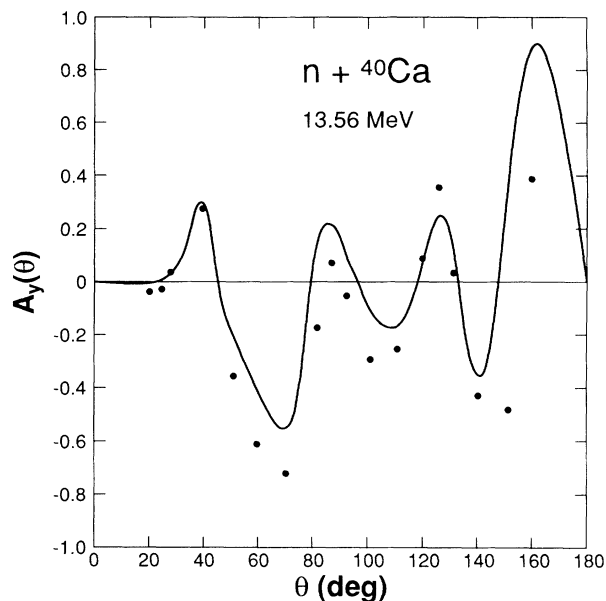


FIG. 8. Comparison of calculated and experimental analyzing powers for  $n + {}^{40}\text{Ca}$  scattering at 13.56 MeV. Experimental data shown are those of Ref. [26].

improve our present model such that detailed agreements with experiment can at least be achieved in the cases where the target nuclei have closed-subshell configurations.

#### IV. SUMMARY AND CONCLUSION

In this investigation, we analyze the neutron + nucleus scattering data with a nonlocal optical model. The real part of the internuclear interaction is obtained by using the prescription of a recently proposed model  $K$  [8] which is a microscopic model based on the resonating-group formulation. A spherical approximation is introduced to treat the cases where the target nuclei have non-closed-subshell configurations. The parameters involved are fixed by using information learned previously from exact resonating-group calculations in the  $n + \alpha$ ,  $n + {}^{16}\text{O}$ , and  $n + {}^{40}\text{Ca}$  systems. The imaginary part used is purely phenomenological. To avoid detailed adjustments, we have simply adopted the imaginary potentials which have already been obtained by other authors in their analyses with the usual local optical model. The influence of the Perey effect, associated with the use of a nonlocal real part, is taken into account by the introduction of an additional multiplicative factor. This latter factor is then chosen in each scattering case by a simple procedure based on a detailed examination in the  $n + {}^{40}\text{Ca}$  case.

The results obtained for the differential scattering cross sections and the analyzing powers in the  $n + {}^{12}\text{C}$ ,  $n + {}^{16}\text{O}$ ,  $n + {}^{28}\text{Si}$ ,  $n + {}^{32}\text{S}$ , and  $n + {}^{40}\text{Ca}$  cases are rather satisfactory. The essential characteristics of the measured angular distributions are well reproduced. A careful inspection of the calculated and experimental results, especially in the analyzing-power case, does indicate that the present model needs to be somewhat refined if detailed agreement

with experimental data is desired. Even so, considering the facts that the real part of the internuclear interaction in this model is explicitly energy independent and that no fine-tuning in the imaginary part is made, we are of the opinion that model *K* is indeed a useful model of great simplicity and the spherical approximation adopted in this calculation constitutes a reasonable simplifying procedure.

The analyzing power is found to have a fairly noticeable dependence on the configuration chosen for the target nucleus. This is an interesting finding, since it suggests that the measurement of this particular quantity may be a way to study nuclear structure by means of elastic-scattering processes. At the present stage, however, we do not think that we can use this information to its full advantage. The reason is that our present model is not yet refined enough to enable us to examine the fine details of the measured angular distributions.

Encouraged by the success of this investigation, we are now prepared to expand the domain of model *K* by considering other subjects of interest. What we have in mind

is to consider the case of inelastic scattering of nucleons by nuclei, and the case of the internuclear interaction between a light ion (i.e., *d*, *t*, or  $\alpha$ ) and a heavier nucleus such as  $^{40}\text{Ca}$  or  $^{208}\text{Pb}$ . In both of these cases, a considerable amount of tedious analytic derivation may have to be performed. However, considering the importance of achieving a microscopic understanding of these processes, we think that these projects are certainly worth pursuing.

#### ACKNOWLEDGMENTS

One of us (T.K.) wishes to thank Professor L. McLerran for the kind hospitality extended to him at the Theoretical Physics Institute of the University of Minnesota. Financial support is provided to T.K. by the Japanese Ministry of Education and is gratefully acknowledged. Also, we wish to thank the Supercomputer Institute at the University of Minnesota for the generous grant of computer time.

- 
- [1] K. Wildermuth and Y. C. Tang, *A Unified Theory of the Nucleus* (Vieweg, Braunschweig, Germany, 1977).
- [2] Y. C. Tang, *Microscopic Description of the Nuclear Cluster Theory*, Lecture Notes in Physics Vol. 145 (Springer, Berlin, 1981).
- [3] H. M. Hofmann, T. Mertelmeier, and W. Zahn, Nucl. Phys. **A410**, 208 (1983).
- [4] Y. Fujiwara and Y. C. Tang, Phys. Rev. C **41**, 28 (1990); Nucl. Phys. **A522**, 459 (1991); Phys. Rev. C **43**, 96 (1991).
- [5] D. R. Thompson, M. LeMere, and Y. C. Tang, Nucl. Phys. **A270**, 211 (1976).
- [6] H. Horiuchi, in *Trends in Theoretical Physics*, edited by P. J. Ellis and Y. C. Tang (Addison-Wesley, Redwood City, California, 1991), Vol. 2.
- [7] See, e.g., T. Ando, K. Ikeda, and A. Tohsaki-Suzuki, Prog. Theor. Phys. **61**, 101 (1970); K. Langanke, Ph.D. Thesis, Universität Münster, 1980; D. Baye and P. Descouvemont, in *Proceedings of the International Symposium on Developments of Nuclear Cluster Dynamics*, Sapporo, Japan, 1988, edited by Y. Akaishi, K. Katō, H. Noto, and S. Okabe (World Scientific, Singapore, 1988).
- [8] T. Kaneko, M. LeMere, and Y. C. Tang, Phys. Rev. C **44**, 1588 (1991).
- [9] R. J. Philpott, Nucl. Phys. **A289**, 109 (1977).
- [10] R. L. Varner, W. J. Thompson, T. L. McAbee, E. J. Ludwig, and T. B. Clegg, Phys. Rep. **201**, 57 (1991).
- [11] F. D. Becchetti and G. W. Greenlees, Phys. Rev. **182**, 1190 (1969).
- [12] J. Rapaport, Phys. Rep. **87**, 25 (1982); J. Rapaport, V. Kulkarni, and R. W. Finlay, Nucl. Phys. **A330**, 15 (1979).
- [13] T. Kaneko, M. LeMere, and Y. C. Tang, Phys. Rev. C **45**, 2409 (1992).
- [14] H. Horiuchi, Prog. Theor. Phys. **64**, 184 (1980).
- [15] C. R. Howell, R. S. Pedroni, G. M. Honoré, K. Murphy, R. C. Byrd, G. Tungate, and R. L. Walter, Phys. Rev. C **38**, 1552 (1988).
- [16] G. W. Greenlees, G. J. Pyle, and Y. C. Tang, Phys. Rev. **171**, 1115 (1968).
- [17] R. C. Barrett and D. F. Jackson, *Nuclear Sizes and Structure* (Clarendon Press, Oxford, 1977).
- [18] D. R. Thompson, M. LeMere, and Y. C. Tang, Nucl. Phys. **A286**, 53 (1977).
- [19] F. G. Perey, in *Direct Interactions and Nuclear Reaction Mechanisms*, edited by E. Clementel and C. Villi (Gordon and Breach, New York, 1963), p. 125.
- [20] N. Austern, Phys. Rev. **137**, B752 (1965).
- [21] W. Tornow, C. R. Howell, H. G. Pfützner, M. L. Roberts, P. D. Felsher, Z. M. Chen, M. Al-Ohali, G. J. Weisel, R. L. Walter, and A. A. Naqvi, J. Phys. G **14**, 49 (1988).
- [22] J. S. Winfield, S. M. Austin, R. P. DeVito, V. E. P. Berg, Z. Chen, and W. Sterrenburg, Phys. Rev. C **33**, 1 (1986).
- [23] J. S. Petler, M. S. Islam, R. W. Finlay, and F. S. Dietrich, Phys. Rev. C **32**, 673 (1985).
- [24] S. T. Lam, W. K. Dawson, S. A. Elbakt, H. W. Fielding, P. W. Green, R. L. Helmer, I. J. van Heerden, A. H. Hussein, S. P. Kwan, G. C. Neilson, T. Otsubo, D. M. Sheppard, H. S. Sharif, and J. Soukup, Phys. Rev. C **32**, 76 (1985).
- [25] Ph. Martin, Nucl. Phys. **A466**, 119 (1987).
- [26] G. M. Honoré, W. Tornow, C. R. Howell, R. S. Pedroni, R. C. Boyd, R. L. Walter, and J. P. Delaroche, Phys. Rev. C **33**, 1129 (1986).
- [27] R. P. DeVito, S. M. Austin, W. Sterrenburg, and V. E. P. Berg, Phys. Rev. Lett. **47**, 628 (1981).
- [28] M. Baba, N. Yabuta, T. Kikuti, and N. Hirakawa, in *Proceedings of the International Conference on Nuclear Data for Basic and Applied Sciences*, Vol. 1, edited by P. G. Young *et al.* (Gordon and Breach, New York, 1985), p. 223; G. Deconninck and J. P. Meulders, Phys. Rev. C **1**, 1326 (1970); M. Thumm, A. Lesiecki, G. Mertens, K. Schmidt, and G. Mack, Nucl. Phys. **A344**, 446 (1980).
- [29] D. G. Foster, Jr. and D. W. Glasgow, Phys. Rev. C **3**, 576 (1971).